A Cellular Automaton / Finite Element model for predicting grain texture development in galvanized coatings

G. Guillemot, M.-N. Avettand-Fènoël, A. Iosta, and J. Foct

Citation: AIP Conference Proceedings **1315**, 727 (2011); doi: 10.1063/1.3552535
View online: http://dx.doi.org/10.1063/1.3552535
View Table of Contents:
http://scitation.aip.org/content/aip/proceeding/aipcp/1315?ver=pdfcov
Published by the AIP Publishing

A Cellular Automaton / Finite Element model for predicting grain texture development in galvanized coatings

G. Guillemot[a], M.-N. Avettand-Fènoël[b], A. Iost[a], J. Foct[b]

[a] *Laboratoire de Mécanique de Lille, UMR CNRS 8107 / Arts et Métiers Paristech - Centre de Lille, 8 boulevard Louis XIV, 59000 Lille*

[b] *Groupe de Métallurgie Physique et Génie des Matériaux, Unité Matériaux Et Transformations, UMR CNRS 8207, Université des Sciences et Technologies de Lille 1, 59655 Villeneuve d'Ascq*

Abstract: Hot-dipping galvanizing process is a widely used and efficient way to protect steel from corrosion. We propose to master the microstructure of zinc grains by investigating the relevant process parameters. In order to improve the texture of this coating, we model grain nucleation and growth processes and simulate the zinc solid phase development.

A coupling scheme model has been applied with this aim. This model improves a previous two-dimensional model of the solidification process. It couples a cellular automaton (CA) approach and a finite element (FE) method. CA grid and FE mesh are superimposed on the same domain. The grain development is simulated at the micro-scale based on the CA grid. A nucleation law is defined using a Gaussian probability and a random set of nucleating cells. A crystallographic orientation is defined for each one with a choice of Euler's angle (ψ,θ,ϕ). A small growing shape is then associated to each cell in the mushy domain and a dendrite tip kinetics is defined using the model of Kurz [2]. The six directions of basal plane and the two perpendicular directions develop in each mushy cell. During each time step, cell temperature and solid fraction are then determined at micro-scale using the enthalpy conservation relation and variations are reassigned at macro-scale. This coupling scheme model enables to simulate the three-dimensional growing kinetics of the zinc grain in a two-dimensional approach.

Grain structure evolutions for various cooling times have been simulated. Final grain structure has been compared to EBSD measurements. We show that the preferentially growth of dendrite arms in the basal plane of zinc grains is correctly predicted. The described coupling scheme model could be applied for simulated other product or manufacturing processes. It constitutes an approach gathering both micro and macro scale models.

Keywords: Galvanizing process, Coupling scheme model, Cellular Automaton, Finite Element
PACS: 81.30.-t

INTRODUCTION

The hot dipping galvanizing process leads to the development of a thin zinc layer at the surface of the steel sheet after immersion in a liquid bath. This process dating from the first half of the 19th century has been considerably improved during the last decades [1] in order to meet the needs of the automotive industry. In this sector industry, continuous galvanizing process enables to protect from corrosion the laminated steel sheet. A coating thickness of 20 to 25 µm is usually obtained after the liquid film solidification [2,3]. Various alloying elements can be added to the bath in order to modify zinc coating appearance and properties. In particular a Fe_2Al_5(Zn)

inhibition layer develops on the steel substrate for an aluminium content of 0.15 to 0.25 wt%. This inhibition layer prevents intermetallic compounds formation and lead to the development of a single η-Zn layer.

Several models have previously been presented to reproduce nucleation and growth processes [3,7]. We propose to develop a coupling scheme model between micro- and macro-scale in order to simulate the solidification of the zinc coating and master its final texture. This model has previously been developed by Gandin and Rappaz [4] to simulate the solidification of the crystallographic cubic orientation alloys. We have adapted this model to the crystallographic hexagonal orientation of zinc grains.

MODEL

The proposed model couples a Cellular Automaton (CA) approach at the secondary dendrite arm scale (*micro-scale*) and a Finite Element (FE) resolution of heat conservation equation at the steel sheet scale (*macro-scale*). Finite element mesh is superimposed to the CA grid of square cells on the whole solidification domain. This CAFE model predicts both grains microstructure evolution and temperature decrease during the solidification process. We present here its major points.

At **macro-scale**, we consider that cooling is mainly due to heat exchange with ambient temperature. Thus, heat flux is modeled using a Fourier condition. Enthalpy variation, ΔH_n^t, at each node n of the macro-scale finite element mesh, is modeled during each macro-time step, Δt, between time t and $t + \Delta t$ as:

$$\Delta H_n^t = -h \left(T_n^t - T_0 \right) \Delta t \qquad (1)$$

where T_n^t and T_0 are the node and ambient temperatures and h is the heat coefficient.

At **micro-scale**, macroscopic enthalpies variations of nodes, ΔH_n, are interpolated in order to estimate enthalpies evolution into each cell of the CA grid, ΔH_ν. For each cell ν, surrounding by nodes n_i, enthalpy evolution is given as:

$$\Delta H_\nu^t = \sum_{i=1}^{N_F} c_\nu^{n_i} \Delta H_{n_i}^t \qquad (2)$$

where $c_\nu^{n_i}$ is the interpolating coefficient between cell ν and node n_i.

Macroscopic and microscopic phenomena correspond to various time variations processes. Thus macroscopic heat evolutions are simulated during macro-time step, Δt, greater than micro-time step, δt. Consequently cell enthalpy evolutions, ΔH_ν^t, (Eq. 2) are then temporally interpolated during each micro-time step between 0 and Δt, in order to estimate enthalpy evolution, δH_ν^t, during each micro-time step. State of each cell is thermodynamically defined with its enthalpy, H_ν^t, its temperature, T_ν^t, and its solid fraction, $g_t^{s\,\nu}$. These parameters are linked through the heat conservation equation.

A set of nucleating cells are previously randomly chosen using a nucleation density, n_{nucl}. In each selected cell, υ, a nucleation undercooling, ΔT_υ, is defined using a Gaussian probability of mean ΔT^μ, and standard-deviation, ΔT^σ. In anticipation of a nucleation process, we define the crystallographic orientation of the grain which could nucleate in each cell of this set. This orientation correspond to a choice of Euler's angle (ψ,θ,ϕ) associated to the seed.

Cells are initially in liquid state. Nodes and cells are at the same temperature, T_i. A growing shape is associated to each cell recovered by the nucleation or the development of a zinc grain (*ie.* mushy domain). This growing shape represents the area fraction of the cell covered by the mushy domain. It is defined as the section of a polyhedron with the substrate plane. This polyhedron corresponds to the three dimensional zinc grain which would not has been prevented to develop in the three dimension (Fig. 1 a). The associated growing shape is consequently a eight-sided polygon (Fig. 1 b).

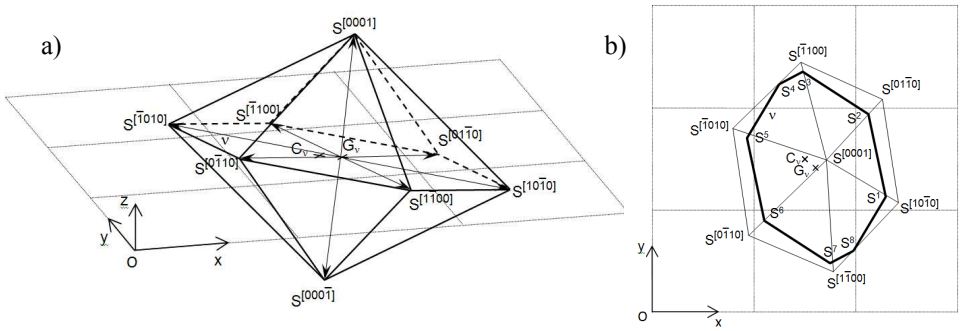

FIGURE 1. a) Representation of the three dimensional zinc grain of the cell ν, with the six dendrite arms of the basal plane (direction $\langle 1\bar{1}00\rangle$) and the two perpendicular dendrite arms (direction $\langle 0001\rangle$). b) Growing shape associated to cell ν (bold lines) corresponding to the section of the polyhedron. The visible faces of the polyhedron are superimposed (thin lines)

If any nucleating cell, υ, is still liquid and the associated nucleation undercooling is reached (ie. $T_\upsilon < T_L - \Delta T_\upsilon$, where T_L is the liquidus temperature), the cell is considered in the mushy domain and an initial growing shape is defined.

Simultaneously, at each micro time step, a dendrite tip kinetics is calculated for each direction <ijkl> of dendrite tips, $v_t^{<ijkl>}$, using the model previously proposed by Guillemot *et al.* [5] corresponding to Kurz *et al.* approach [6] without thermal gradient. For each cell, ν, this kinetics is a function of the cell temperature, T_ν^t and alloy properties. Consequently, in each cell of the mushy domain, the six dendrites arms of the basal plane and the two perpendicular dendrite arms develop. The growing shape associated to each cell get bigger. If this new growing cell engulfs the cell centre of a liquid cell, this cell becomes mushy. A new growing shape is associated to this cell corresponding to the same orientation angle (*ie. Euler's angle*) than the initial one (Fig. 2).

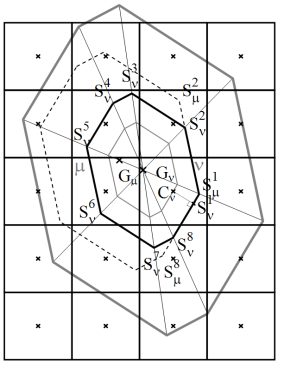

FIGURE 2. The growing shape (dashed lines) associated to cell μ recovers the centre of cell ν, C_ν. A homothetic growing shape is defined for the new mushy cell (bold lines). Capture and maximal growing shape are also defined (bold and thin grey lines).

Maximal and capture growing shape enable to define the current volume fraction of mushy domain into each cell, g_ν^m at any micro time step. If the cell recovers its entire neighborhood, the volume fraction is equal to one. The solid fraction of the mushy domain, g_ν^{sm}, and temperature, T_ν, are links through the solidification path:

$$\begin{aligned} &\text{if } g_\nu^m < 1 \quad g_\nu^{sm} = \frac{1}{1-k}\frac{T_L - T_\nu}{T_M - T_\nu} && \textit{(level rule)} \\ &\text{if } g_\nu^m = 1 \quad g_\nu^{sm} = 1 - \alpha\left(\frac{T_M - T_\nu}{T_M - T_L}\right)^{\frac{1}{k-1}} && \textit{(Scheil's rule)} \end{aligned} \tag{3}$$

where T_M is the melt temperature.

The solid fraction of cell ν, g_ν^s, is then defined as the product of the volume fraction and solid fraction of the mushy domain. Considering the heat conservation equation, we can then define the solid fraction and temperature of cells at the end of each micro time step. Temperature and solid fraction of cells are then reassigned at macroscopic scale in order to estimate new temperature and solid fraction of nodes. Theirs variations during macro time step are calculated as:

$$\Delta\xi_n^t = \frac{1}{\Lambda_n}\sum_{i=1}^{N^n} c_{\nu_i}^n \Delta\xi_{\nu_i}^t \tag{4}$$

where $\xi \in \{T, g^s\}$, Λ_n is a normalization parameter and N^n is the number of cells, ν_i, surrounding node n.

At the end of each macro-time step, thermodynamic state of cells (micro-scale) and nodes (macro-scale) are defined. The new enthalpy variations at macro-scale can then be estimated (Eq. 1). The coupling scheme model enables to deduce macro-scale temperature and solid fraction evolution from the micro-scale solidification process.

RESULTS

We have developed the present model in order to simulate the grain structure evolution for successive cooling times and compare the final texture to EBSD measurement. These measurements have been conducted on a domain of 1.482×2.088 mm^2 (Fig. 3 a) of a galvanized steel sheet for a Zn-0.23 wt % Al alloy. The grain density is equal to 1.5×10^7 m^{-2}. Crystallographic orientations have been measured on the 46 visible grains of the sample. These measurements have indicated that crystallographic orientations (ψ,ϕ) for Euler's angle are both randomly distributed. We have also measured the nutation angle, θ, evolution (Fig. 3 b) corresponding to the angle between the <1000> direction and the normal to the sample. The classes [22.5°;45°] and [45°;67.5°] are close to the random distribution. Nevertheless, a small texture is noticeable for small θ angle. This result is close to the one presented by Sémoroz [7]. Moreover an unambiguous texture of the inhibition layer Fe_2Al_5 has been proven by Mössbauer spectroscopy [8,11].

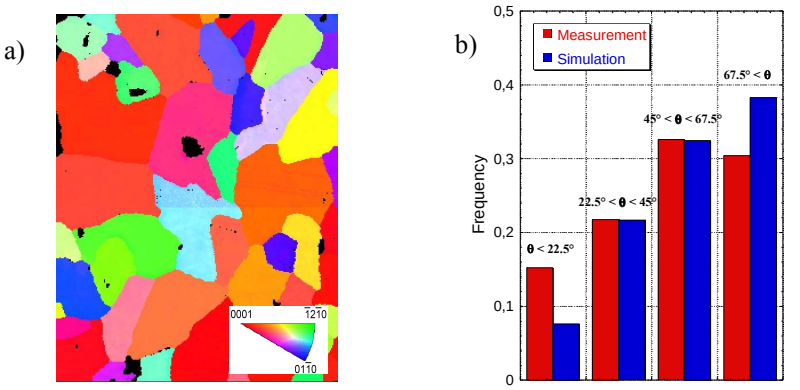

FIGURE 3. a) Grains texture of the galvanized steel sample obtained with EBSD measurements. Some measurements have failed (black domain). b) Nutation angle, θ, distribution for step of 22,5 °

We have simulated grains development considering a randomly distribution of Euler's angle. Galvanizing process is conducted from liquidus temperature. A greater surface (4.446×6.264 mm^2) than the analyzed one is considered. Nucleating parameters (ΔT^{μ}, ΔT^{σ}) are equal to (0.5 °C,0,25 °C). Cell size of the CA grid is of 10 µm. Substrate and liquid layer thicknesses are of 1.3 mm and 10 µm. Properties of the alloy can be found in [7,9,10]. Fig. 4 a) presents grain structure evolution during cooling at various times. We define the Grain Enlargement Factor (GEF) as the ratio of the surface fraction of grains belonging to an orientation angle class to their frequency on the sample. GEF evolutions show the ability for a specific orientation angle to favour the grain development. GEF measurements on galvanized steel sheet sample have been compared to simulation for each of the four nutation orientation angle classes (Fig. 4 b). We show same decreases of GEF with the θ angle increase. The expected preferential growth of zinc grain in their basal plane is well reproduced. New measurements should improve the comparison. Likewise nucleation process and kinetics parameters should also be enhanced.

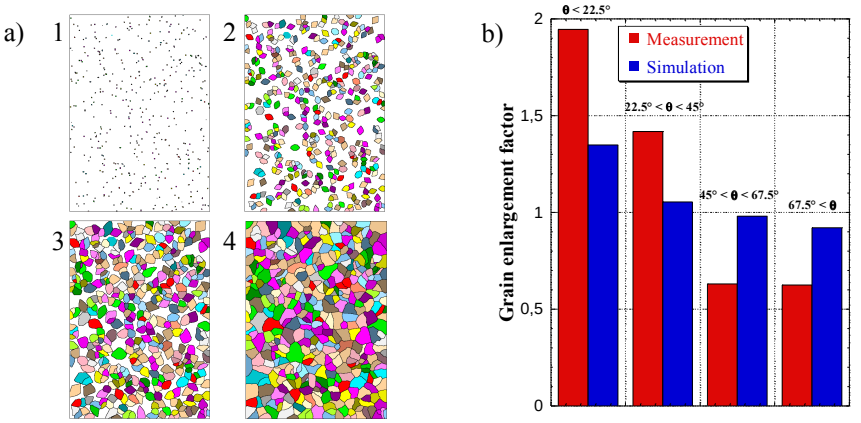

FIGURE 4. a) Grain structure evolution for various cooling times (1 : t = 0,12 s; 2 : t = 0,15 s; 3 : t = 0.17 s; 4 : t = 0.25 s) b) GEF comparison for the various nutation orientation angle classes.

CONCLUSION

An adaptation of the CAFE coupling scheme model has been proposed to model the development of zinc grain coating in galvanizing process. A random distribution of initial grain orientation has been applied, close to EBSD measurement. A dendrite tip growth kinetics has been defined for each growth direction of basal plane and perpendicular to basal plane.

The decrease of the GEF with the increase of the nutation orientation angle has been reproduced. Zinc grains preferentially growth in their basal plane. The small analysis surface should lead to conduct new measurements in order to improve simulation parameters and coating texture prediction.

ACKNOWLEDGMENTS

The authors would like to thank the International Lead Zinc Research Organization (ILZRO) for the financial support supplied to this research project.

REFERENCES

1. J. Lamesch, *Histoire mondiale de la Galvanisation*, Publication Arcelor, (2003)
2. J. Strutzenberger and J. Fardel, *Metall. Mater. Trans. A*, **29**, 631-646 (1998)
3. A. Poulon-Quintin, A. Chirazi, G. Reumont, J. Foct, F. Goodwin, Galvatech'04, Conference Proceedings, 691-702 (2004)
4. Ch.-A. Gandin, M. Rappaz, *Acta Metall. Mater.*, **42**, n°7, 2233-2246 (1994)
5. G. Guillemot, Ch.-A. Gandin, H. Combeau, *ISIJ Inter.*, **46**, 880-895 (2006)
6. W. Kurz, B. Giovanola, R. Trivedi, *Acta Metall.*, **34**, 823-830 (1986)
7. A. Sémoroz, L. Strezov, M. Rappaz, *Metall. Mater. Trans. A*, **33**, 2685-2694 (2002)
8. J. Foct, M.N. Avettand-Fènoël, Galvatech '07, Conference Proceedings, 327-332 (2007)
9. A. Sémoroz, S. Henry, M. Rappaz, *Metall. Mater. Trans. A*, **31**, 487-495 (2000)
10. P. Perrot, J.-C. Tissier, J.-C. Dauphin, *Zeit. für Metall.*, **83**, 786-790 (1992)
11. M.-N. Avettand-Fenoel, C. Cordier-Robert, G. Guillemot, F. Goodwin, J. Foct, *Hyperfine Interactions*, **190**, n°1-3, 29-36 (2009)